

Initial nano-tomo-ptychography 3D-imaging results on the SWING beamline at Synchrotron SOLEIL

Christer Engblom^{1,a}, Yves-Marie Abiven¹, Filipe Alves¹, Felisa Berenguer¹, Thomas Bizien¹, Arnaud Gibert¹, Florent Langlois¹, Alain Lestrade¹, Javier Pérez¹

¹Synchrotron SOLEIL, St Aubin, France

^achrister.engblom@synchrotron-soleil.fr

Abstract

A nanoprobe end-station was previously (2018) installed and validated on the SWING beamline (Synchrotron SOLEIL) for 2D-nano-ptychography with an imaging resolution of 40 nm. As a continuation of the project, this very system has recently been upgraded to allow for (1): 2D-imaging resolutions of 20 nm or better, and (2): 3D- nano-tomo-ptychography imaging with spatial resolutions of 50 nm or better. Additionally, the system has been designed to be portable and capable of handling sample-sizes from the micrometer scale to several hundreds of a micrometer. The end-station actuated a total of 11 Degrees Of Freedom (DOF) composed of a sample stage (5 DOF), an optical stage comprised of central stop- and Fresnel zone plate optical elements (3 DOF), as well as an order sorting aperture stage (3 DOF). All positioning stages were comprised of piezo-driven actuators or high-quality brushless motors, of which synchronized control (with kinematic modelling) was done using the SOLEIL Delta Tau platform. In addition, interferometry feedback was used for reconstruction purposes. Imaging results are promising: the system was able to resolve 2D-images with a resolution better than 19 nm measured with a Siemens star, and 3D- images with a spatial resolution of 40 nm using a Silica sample.

Keywords: Synchrotron SOLEIL, ptychography, tomography, nanoprobe, nanopositioning, Delta Tau, control, kinematic modelling, interferometry

1. Introduction

The Nanoprobe Project[1, 2], a 4-year joint collaboration between Synchrotron SOLEIL and MAXIV (Sweden), was launched in 2013 in order to produce a 3D scanning-nanoprobe prototype. After the project had ended in december 2016, a SOLEIL-based team dedicated to nano-positioning systems was formed (*Nanoprobe-SOLEIL*).

In preparation for the upcoming SOLEIL Synchrotron upgrade [4] (which will utilize a more coherent light source) and to address a growing need amongst its users, the SWING beamline [3] at Synchrotron SOLEIL has decided to add high-resolution coherent diffractive imaging, ptychography, to its roster of experimental setups. And as such, the SWING beamline has now staked out the following long-term goals for its nanoprobe end-station:

1. *System portability*: to keep a level of flexibility between different type of experiments, any new system needs to be compact and capable of installing/uninstalling to/from the beamline within a few hours.
2. *Nano-2D-ptychography*: imaging resolution equal to or better than 20 nm, with full-range scans of 10² μm up to several 100² μm .
3. *Nano-3D-tomo-ptychography*: spatial resolution equal to or better than 50 nm, with full-range scans of 10³ μm up to several 100³ μm

Goals 1 and 2 were partially accomplished at the end of 2018, where a new portable Nanoprobe endstation performed nano-2D-ptychography [1] at a resolution of 40 nm.

The scope of the project continuation (and the subject of this paper) is therefore to: upgrade the Nanoprobe end-station to allow for higher 2D-imaging resolution, and to introduce and test nano-3D-tomo-ptychography at the SWING beamline.

The term *Nanoprobe End-Station* will in this paper be referred to the support and environment that houses the active parts used

in scans. The term *Nanoprobe System* will refer to the Nanoprobe End-Station as well as all its driving electronics & control systems.

2. Nanoprobe end-station overview

The new end-station can be sectioned up into four main parts; the overall system support structure (including plexiglass cover), the interferometer support structure, an actuated sample stage, and actuated optical stages. The optical stages are composed of a Fresnel-Zone-Plate & Central-Stop Stage (FZP-CS), and an Order-Sorting-Aperture (OSA) Stage. Figure 1 illustrates the setup, showing each stage and their respective Degrees-of-Freedom (DOF).

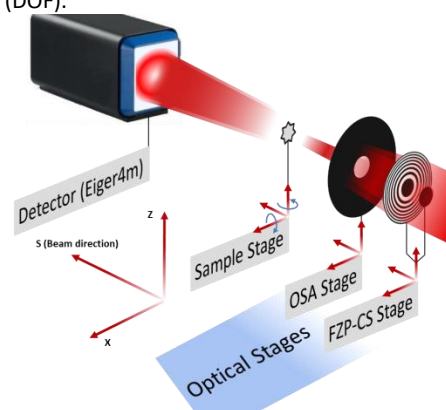


Figure 1. Principal scheme outlining the SXZ-orientation of the Nanoprobe End-Station stages and their respective degrees of freedom.

2.1. Metrology analysis & system design

A metrology analysis was carried out to identify key parameters for the mechanical design. A high resolution nano-2D step-scan would, for an example, necessitate differential positional tracking data between the Sample- and FZP-CS- Stages at each step of detector-image-acquisitions. Interferometer

position-tracking was consequently installed along the (X, Z)-directions for both stages – the sensors were always installed in pairs (or triples) to provide additional angular displacements feedback.

Introducing nano-3D-tomography-ptychography requires – almost by definition – a rotation drive along the R_z -axis on the Sample Stage; this poses a problem when utilizing interferometry position-tracking from the sides (ex. X-direction). The typical use of a cylindrical (or spherical) mirror for sample-tracking during full R_z -rotations does not give satisfactory results due to the apparition of interferometric sensor nonlinearities; a planar mirror in the X-direction was therefore used (lower nonlinearity levels with interferometry readings). In ptycho-tomography, the 3D position of the sample can be managed by the reconstruction algorithm for the (X, Z) translations. In other words, the use of a cylindrical mirror is not mandatory and as a main consequence, the runout of the rotary stage does not pose a problem provided that the runout-amplitude meets the constraint of the scan size.

Another issue with high resolution nano-3D-tomography-ptychography is that wobble along the sample-Rx-axis needs to be managed for each movement along the Rz-axis; this is due to defects (error motions) in the Rz rotational drive. Wobble management in the R_s -direction was not necessary in this experiment because the X sensors are set up at the same height level as the sample.

2.2. Supports & environment

The nanoprobe upgrade had its system stage support reworked (in a one-piece aluminium) to have a smaller footprint and therefore higher level of rigidity (See Fig. 2). In addition, the interferometer support structure was completely redone to allow for the 9 interferometer sensors to be mounted from the top as well as the sides. Compromises were made in the conception of the support structures in order adhere to beamline specifications.

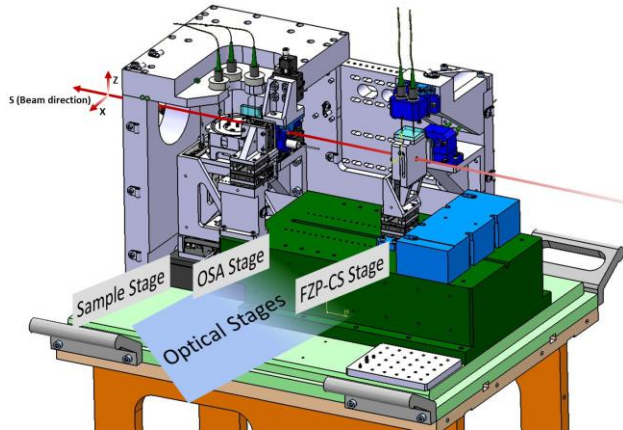


Figure 2. 3D model of the Nanoprobe stage support & environment. This particular image is shown without its plexiglass cover, which is added during scans for thermal stabilisation and to minimize air turbulence.

2.3. Optical stages

The optical stages consists of two main elements: the Fresnel-Zone-Plate-Central-Stop (FZP-CS) stage; and the Order-Sorting-Aperture (OSA) stage. These stages each actuate into three linear DOF in the SXZ- space, using three stacked encoded linear piezo-multi-leg positioners, allowing for high-resolution (0.5 nm) and long-range movements in the millimetre range. In addition, the FZP-CS stage is equipped with 4 interferometer sensors (see Fig. 3) for position tracking in the (X, Z, R_x , R_z) – space.

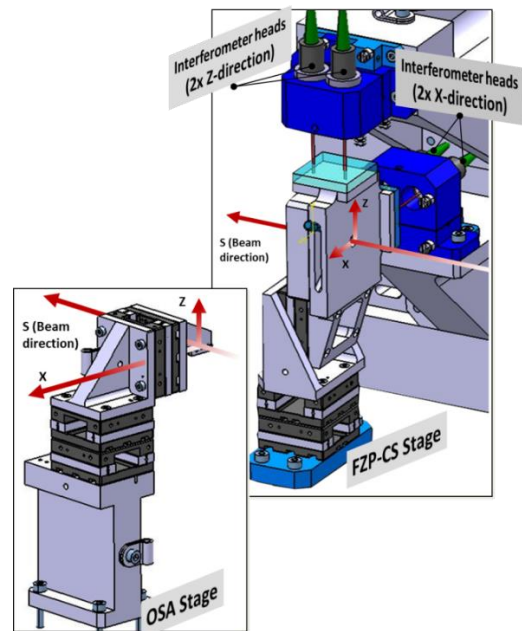


Figure 3. 3D model of: (left) Order-Sorting-Aperture (OSA) Stage, (right) Fresnel-Zone-Plate-Central-Stop (FZP-CS) Stage. Both stages annotated with its three DOF. Note that the FZP-CS stage includes four interferometer sensors (that are all mounted on a separate support structure) to measure (X, Z, R_x , R_z)- tracking for image reconstruction purposes.

2.4. Sample stage

The sample stage consists of 5 axes that actuate into the (S, X, Z, R_x , R_z) – space; comprised of high resolution (1 nm) and long-range (>10 mm) linear SXZ- drives, a high- precision (with repeatable runout errors < 200 nm [2]) full-range rotational R_z -drive, as well as a short-range high-resolution R_x -actuator. 2D-ptychography scans would involve incremental nanometer (deca- or hundreds of nm) displacements on the XZ- plane (over a range of up hundreds of μ m). Figure 4 shows the setup of the sample stage, here with an overlying bracket holding interferometer sensors for sample tracking during scans. Interferometer measurements would only be used for tracking movement errors for post-process image corrections.

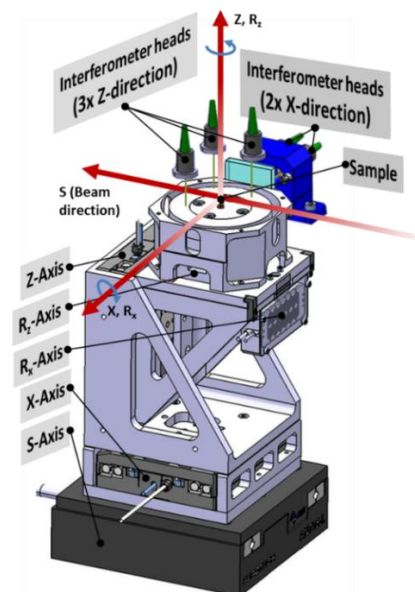


Figure 4. 3D model of the Sample Stage, here annotated with its five DOF. Also shown, five interferometry sensors (that are all mounted on a separate support structure) providing (S, Z, R_x , R_z) – positional tracking for image reconstruction purposes.

3. Control & Data Acquisition

3.1. System architecture

Figure 5 shows a detailed system architecture of the Nanoprobe end-station where 4 Delta Tau PowerPMAC-based controllers (Soleil high-end controller from the REVOLUTION project [4, 5]) are interfaced with all motorised axes and interferometer channels. All in all, the following setup is used:

1. Two controllers, that are interlinked (Delta Tau MACRO interface [7]), handles closed-loop control of the 11 axes in the Sample- and Optical Stages.
2. Two controllers, also interlinked via the MACRO bus, are interfaced with 9 interferometer channels from the Sample- and – Optical Stages. These controllers are only used for position tracking and capture, and provide detector-synchronized (via a low-level TTL trigger signal) interferometer positional data for image reconstructions.

All scans and user commands operate through the TANGO control system [8], interfacing directly with the Delta Tau controllers via the beamline network. The SWING beamline, in this case, makes use of the Passerelle platform [9] (which operate through the TANGO system) to launch the 2D- and 3D-scans.

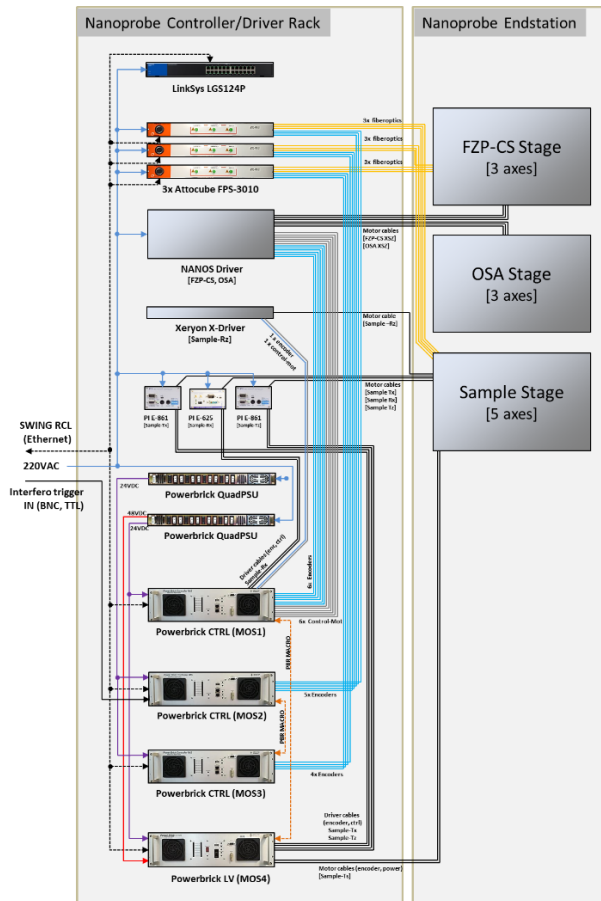


Figure 5. Control/Acquisition architecture, from/to the Nanoprobe end-station to/from the users via the electronics and high-level software (TANGO).

3.2. Control- & data acquisition schemes

Figure 6 shows a simplified scheme of the nanoprobe control- and data acquisition. As was mentioned in Section 3.1, the control and data acquisition systems are kept separated at the low level; meaning that no interferometer feedback is used in low-level closed-loop control – instead they are almost entirely used as a reference point for image reconstructions. In the case

of Rx-compensation (as was mentioned in Section 2.1), interferometry feedback-control is applied via the TANGO layer.

Control and acquisition strategies can be divided into the following:

- *Control Strategy, Sample Stage (5 axes)*: All 5 axes can be controlled using multi-axial synchronization (via kinematic models) – this can be used to keep the rotational axes at the center of the sample when possible. Ex: the user could dynamically change the axis of rotation R_z (i.e recenter the sample) using only the linear stages below the rotation stage, and therefore have no need to physical drives on top of the rotation. stage.
- *Control Strategy, Optical Stages (6 axes)*: A stacked SXZ-design allows for separate control of each axis with a high-frequency PID regulation.
- *Position Capture Strategy, interferometer data (9 channels)*: position tracking and capture of all channels are synchronized (and averaged from pulse duration) via a low-level TTL trigger signal, and are automatically processed via kinematic models to provide (X, Z, R_s, R_x, R_z) – data for the Sample stage (R_s -tracking would in this case not be used actively in the scans), and (X, Z, R_x, R_z) – data for the FZP-CS stage.

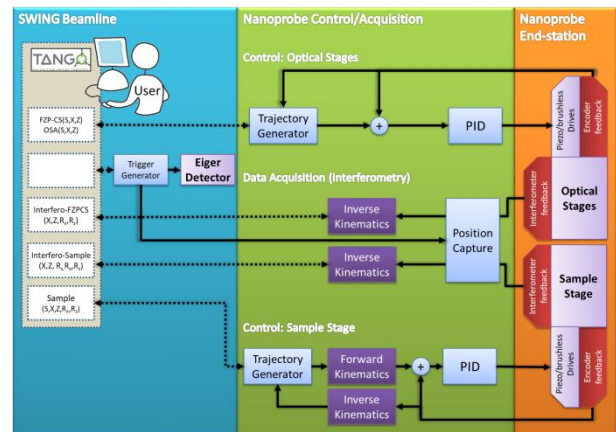


Figure 6. Simplified system control/data acquisition scheme: optical stage closed-loop control is achieved via PID regulation with encoder feedback, sample stage control uses PID regulation with kinematic models to keep all axes rotations centered on the sample position. Interferometer position capture is synchronized via a trigger generator with the Eiger detector.

4. Imaging results

Figure 7 shows the reconstructed 2D phase image of a Siemens Star sample, where it was able to resolve the innermost 20 nm spoke distance. The system resolution was furthermore assessed by image comparisons (see Fig. 8) using the Fourier Shell Reconstruction (FSC) method [10], where it is shown that a resolution better than 17 nm was achieved.

Figure 9 shows a mid-slice of a 3D-tomography scan (in this case, showing electron density) of a Silica sample, where the internal submicronic cavities are evident. 3D spatial resolution (using FSC correlation) was calculated to be (see Fig. 10) below 40 nm.

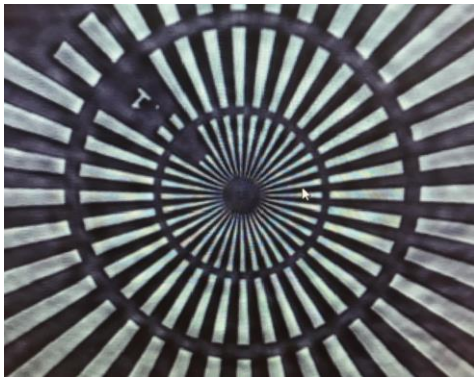


Figure 7. The reconstructed 2D phase image of a Siemens Star, here focusing on the center of the sample - the image resolves the innermost 20nm spokes of the Siemens star.

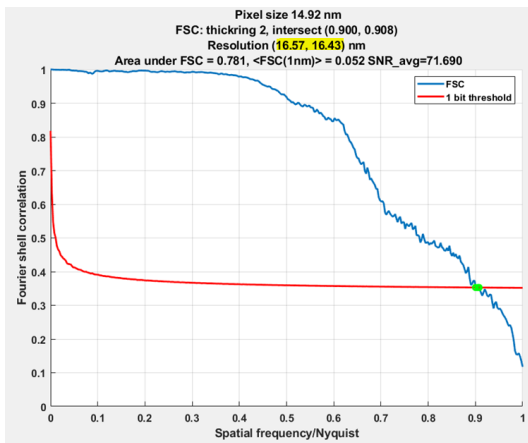


Figure 8. 2D image resolution (or image repeatability) is estimated by two-image comparisons using Fourier Shell Correlation with an FSC 1-bit cutoff criteria – one can see that the resolution (marked yellow) is estimated to be less than 17 nm.

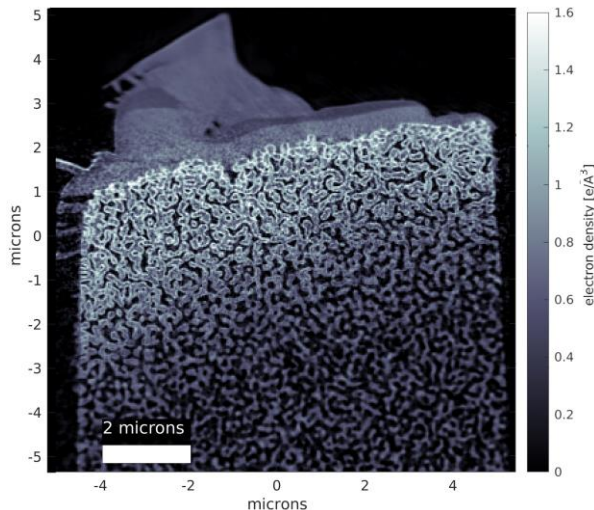


Figure 9. Mid-slice of a 3D tomogram showing electron density [e/A^3] of a Silica sample – one can see the nanometer-sized cavity interior structure.

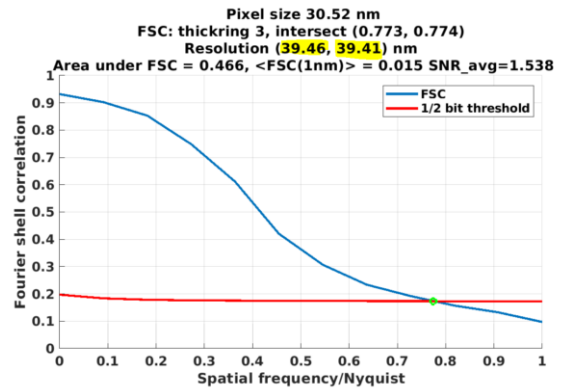


Figure 10. 3D spatial resolution (or image repeatability) is estimated by two-image comparisons using Fourier Shell Correlation with an FSC 1/2-bit cutoff criteria – one can see that the resolution (marked yellow) is estimated to be less than 40 nm.

5. Summary & Conclusion

The new Nanoprobe end-station has been upgraded to allow for a better 2D imaging resolution whilst introducing the possibility of nano-3D-tomo-ptychography scans. The results have been very promising; 2D-imaging resolutions have been shown to be less than 17 nm, whilst 3D-imaging spatial resolutions to be better than 40 nm.

Acknowledgements

Data processing was carried out using the cSAXS ptychography MATLAB package developed by the Science IT and the coherent X-ray scattering (CXs) groups, Paul Scherrer Institut, Switzerland."

References

- [1] C. Engblom, Y-M. Abiven, F. Alves, F. Berenguer, T. Bizien, A. Gibert, F. Langlois, A. Lestrade, P. Montaville, J. Pérez, "2D-Nano-Ptychography Imaging Results on the SWING Beamline at Synchrotron SOLEIL", presented at the 17th Int. Conf. on Accelerator and Large Experimental Physics Control Systems (ICALPECS'19), New York, NY, USA, Oct. 2019, paper MOCPL06
- [2] C. Engblom, Y-M. Abiven, F. Alves, F. Berenguer, T. Bizien, A. Gibert, F. Langlois, A. Lestrade, P. Montaville, J. Pérez, "Nanoprobe results: metrology & control in stacked closed-loop systems", in Proc. ICALPECS2017, Barcelona, Spain, Oct 2017, pp. 1028-1033. doi:10.18429/JACoW-ICALPECS2017-WEAPL04
- [3] SWING Beamline at Synchrotron SOLEIL, <https://www.synchrotron-soleil.fr/en/beamlines/swing>
- [4] A. Loulergue et al., "Baseline lattice for the upgrade of SOLEIL", in Proc. IPAC'18, Vancouver, BC, Canada, Apr.-May 2018, pp. 4726-4729. doi:10.18429/JACoW-IPAC2018-THPML034
- [5] Delta Tau, <http://www.deltatau.com>
- [6] S. Zhang et al., "Revolution Project: Progress in the Evolution of Soleil Motion Control Model", in Proc. ICALPECS2015, Melbourne, Australia, Oct. 2015, pp. 201-204. ISBN978-3-95450-148-9
- [7] Delta Tau MACRO interface, <http://www.macro.org/index-1-1.html>
- [8] Tango Control Systems, <https://www.tango-controls.org/>
- [9] Passerelle Platform, <https://supportsquare.io/passerelle-platform/>
- [10] M. Van Heel, M. Schatz, "Fourier shell correlation threshold criteria", in J. Struct. Biol. 2005 pp. 250-262.